doi:10.1093/brain/awl232 *Brain* (2007), **130**, 548–560

The extent of resection of FDG-PET hypometabolism relates to outcome of temporal lobectomy

Anita B. Vinton,[1] Ross Carne,[1] Rodney J. Hicks,[2] Patricia M. Desmond,[1] Christine Kilpatrick,[1] Andrew H. Kaye[1] and Terence J. O'Brien[1]

[1]The Departments of Medicine, Surgery, Radiology and Neurosciences, The Royal Melbourne Hospital, The University of Melbourne, Parkville and [2]Centre for Molecular Imaging, Peter MacCallum Cancer Centre, East Melbourne, Victoria, Australia

Correspondence to: Dr Anita Vinton, The Department of Medicine, The University of Melbourne, Royal Parade, Parkville, Victoria 3050, Australia
E-mail: abvinton1@optusnet.com.au

A significant minority of patients undergoing surgery for medically refractory non-lesional temporal lobe epilepsy (TLE) continue to have seizures, but the reasons for this are uncertain. Fluorodeoxyglucose (FDG) PET shows hypometabolism in a majority of patients with non-lesional TLE, even in the absence of hippocampal atrophy. We examined whether the extent of resection of the area of FDG-PET hypometabolism influenced outcome following surgery for non-lesional TLE. Twenty-six patients who underwent temporal lobectomy for medically refractory TLE with at least 12 months follow-up were studied. The preoperative FDG-PET was compared with 20 non-epileptic controls using SPM99 to identify regions of significant hypometabolism ($P < 0.0005$, cluster > 200). This image was then co-registered to the postoperative MRI scan. The volume of the FDG-PET hypometabolism that lay within the area of the resected temporal lobe was calculated. The volume of temporal lobe resected was also calculated. Patients with a good outcome had a greater proportion of the total FDG-PET hypometabolism volume resected than those with a poor outcome (24.1% versus 11.8%, $P = 0.02$). There was no significant difference between the groups in the volume of temporal lobe resected ($P = 0.86$). Multivariate regression demonstrated that the extent of resection of the hypometabolism significantly correlated with outcome ($P = 0.03$), independent of the presence of hippocampal sclerosis ($P = 0.03$) and total brain volume of hypometabolism ($P = 0.45$).

The extent of resection of the region of hypometabolism on the preoperative FDG-PET is predictive of outcome following surgery for non-lesional TLE. Strategies that tailor resection extent to regional hypometabolism may warrant further evaluation.

Keywords: temporal lobe epilepsy; FDG-PET; temporal lobectomy outcome

Abbreviations: AED = anti-epileptic drug; AH = amygdalohippocampectomy; ATL = anterior temporal lobectomy; FDG = fluorodeoxyglucose; HS = hippocampal sclerosis; ROI = region of interest; SPM = statistical parametric mapping; TLE = temporal lobe epilepsy

Received February 25, 2006. Revised July 28, 2006. Accepted August 1, 2006. Advance Access publication September 7, 2006.

Introduction

Temporal lobe epilepsy (TLE) is the most common focal epilepsy syndrome in adults that is refractory to medical treatment. Surgical treatment offers the best chance of seizure freedom in these patients (Wiebe *et al.*, 2001). Even in carefully selected patients, however, a significant minority continue to experience seizures after surgery. Unfortunately, this group remains difficult to define preoperatively. A better understanding of preoperative prognostic indicators may

allow more appropriate selection of patients for surgery and improved surgical strategies to optimize postoperative outcomes.

Fluorodeoxyglucose (FDG) PET scans have been demonstrated to reliably lateralize seizure focus in mesial TLE, with decreased glucose uptake in the epileptogenic temporal lobe (Theodore *et al.*, 1983). The pathophysiological basis for this hypometabolism remains elusive, and various theories have been proposed. It has been postulated to relate to underlying cell loss; however, a number of studies have not found a strong correlation with hippocampal volume loss or neuronal cell counts (Henry *et al.*, 1994; Semah *et al.*, 1995; O'Brien *et al.*, 1997). Other aetiological theories proposed include neuronal dysfunction—possibly as an effect of repeated seizures, synaptic reorganization and neuronal sprouting.

While it is generally believed that the region of hypometabolism is larger than the epileptogenic zone, no previous study has systematically examined whether the extent of its resection is related to post-surgical outcome. If the basis for the decreased glucose metabolism is related to underlying epileptic neuronal dysfunction, then excision of this area, either in total or in part, may impact seizure freedom rates. We hypothesized that there is a relationship between the outcome from temporal lobectomy surgery for medically refractory TLE and the extent of resection of the hypometabolism on the preoperative FDG-PET. This study was designed to examine this relationship.

Various studies have examined the relationship of FDG-PET to seizure freedom postoperatively, and several prognostic indicators have been reported (Griffith *et al.*, 2000; Koutroumanidis *et al.*, 2000; Newberg *et al.*, 2000; O'Brien *et al.*, 2001; Choi *et al.*, 2003). However, these studies have all just related the presence or site of the hypometabolism to outcome, but not the relationship to the extent of resection of the hypometabolism. Furthermore, these papers have largely relied on visual interpretation of the FDG-PET scans, which can be confounded by inter-interpreter variability, and does not allow quantification of the hypometabolic regions. In addition, FDG-PET scans are unable to accurately localize intracerebral structures, making exact anatomical localization of hypometabolism difficult.

Statistical parametric mapping (SPM) is a voxel-based approach to the analysis of FDG-PET data, which allows comparisons of individual voxels to those in a normal brain, and thus quantification of hypometabolism. This removes inter-observer confounders. Co-registration with the patient's anatomical MRI allows more accurate anatomical localization of the SPM-identified regions of hypometabolism. In this study, we applied these methods to quantify the volume of the region of FDG-PET hypometabolism and examined the relationship between the percentage included in the surgical resection and the outcome with respect to seizures. We also used co-registration of the postoperative to the preoperative MRI to determine the volume of temporal lobe resected, and whether this was independently associated with surgical outcome.

Material and methods

Patients and clinical details

The study group consisted of 26 patients with medically refractory TLE who had undergone temporal lobectomy between 1998 and 2003. Patients were selected consecutively from the epilepsy monitoring unit database and were considered eligible if a preoperative FDG-PET scan demonstrating a region or regions of focal hypometabolism was available as part of their pre-surgical evaluation. Determination of the presence of focal hypometabolism was performed using the quantitative SPM-based method detailed below in Post-acquisition FDG-PET image processing.

Pre-surgical evaluation included neurological examination, brain MRI, interictal FDG-PET, video EEG monitoring and neuropsychological assessment. Where possible, ictal and interictal brain single photon emission computed tomography (SPECT) was also performed. The presence or absence of hippocampal sclerosis (HS) on MRI scans was determined by expert neuroradiologists at our epilepsy centre using accepted criteria, particularly the presence of unilateral atrophy and increased T_2-signal of the hippocampus. Patients with other temporal lobe pathology visible on MRI were excluded. The diagnosis and lateralization of TLE was confirmed on the basis of these investigations. Selection for surgery in patients with a normal MRI required well-lateralized ictal events with concordant lateralization on interictal FDG-PET, and no discordant information from other modalities, such as SPECT or neuropsychological assessment. Four patients had chronic intracranial EEG recordings with surgically implanted subdural grid electrodes to confirm the epileptogenic zone before undergoing the temporal resection.

All patients subsequently underwent a tailored standard anterior temporal lobectomy (ATL). One of two surgeons performed each of the operative procedures. The anterior temporal lobe was removed, with an en bloc excision of neocortical structures, followed by microsurgical resection of the amygdala, and subsequent complete en bloc resection of the hippocampus and parahippocampal gyrus. The extent of hippocampal resection was standardized for all patients and confirmed on the postoperative MRI. Patients with a non-dominant lobe resection had excision of 4 cm of the superior and middle temporal gyrus, and 5–6 cm of the inferior temporal gyrus or to the vein of Labbe. Patients undergoing a dominant lobectomy had the superior temporal gyrus left intact, and the middle and inferior temporal gyrus was excised 4–5 cm, or to the vein of Labbe. All patients were followed up for at least 12 months postoperatively. An MRI scan was also performed at least 3 months postoperatively.

Following surgery, all patients had a standardized approach to their anti-epileptic drug (AED) therapy management. No changes were made in the first 6 months postoperatively. Patients on three or more AEDs were then weaned to two AEDs by 1 year, to one AED by 2 years, and then this drug was continued indefinitely. In patients who had seizure recurrence, AED therapy was increased and tailored to their individual response.

Postoperative outcome with respect to seizures was graded according to a 12-point seizure frequency score (Table 1; Engel *et al.*, 1993) that we have used in previous studies (O'Brien *et al.*, 1998*b*, 2000, 2001). Patients were considered to have a good

Table 1 Seizure frequency scale

Seizure frequency	Score
Seizure-free, no AEDs	0
Seizure-free, need for AEDs unknown	1
Seizure-free, needs AEDs	2
Non-disabling simple partial seizures	3
Non-disabling nocturnal seizures only	4
Number of disabling seizures	
1–3 per year	5
4–11 per year	6
1–3 per month	7
1–6 per week	8
1–3 per day	9
4–10 per day	10
>10 per day	11
Status epilepticus	12

outcome with a score of <5 (i.e. seizure freedom, nocturnal seizures only or up to three seizures per year). A good outcome is equivalent to a Class I and II outcome on the Engel scale. Outcome was determined from state of seizure control at latest follow-up.

The study was approved by the Human Research Ethics Committees of Melbourne Health, St Vincent's Hospital and The Peter MacCallum Cancer Institute.

FDG-PET acquisition

Interictal out-patient FDG-PET scans were acquired on a PENN PET 300H Tomograph scanner as described previously (O'Brien *et al.*, 2001). A three-dimensional whole-head acquisition was performed with a 25-cm field of view. For the 2 mm slice thickness used for whole-body imaging, the measured resolution was 4.2 mm at full width at half maximum transaxially and 5.4 mm at full width at half maximum out of plane. All patients were fasted for 4 hours before scanning and rested in a quiet, darkened room with eyes open and ears unoccluded for 30 min before FDG administration, and for at least 30 minutes afterward. Scanning commenced 5–60 min after 37–111 MBq (1–3 mCi) of FDG was administered. Although this represents a lower administered activity than used with current generation scanners, this dose is sufficient to yield adequate statistical quality studies on a 3D NaI detector-dedicated PET scanner. The acquisition time was 30–40 min, achieving total counts of >40 million. The images were reconstructed into a 256 × 256 mm cylindric volume with a 2 mm slice thickness. The reconstruction process created a standard series of contiguous images oriented in the transaxial, coronal, sagittal and transtemporal planes. Routine EEG monitoring was not performed during the scan.

Interictal PET scans were also obtained using an identical protocol in 20 healthy volunteers (10 males, 10 females, median age: 32, range: 20–57) who served as control subjects. There was no history of neurological disease or intake of medications known to affect FDG-PET studies. All volunteers gave written consent.

MRI acquisition

All MR scans were performed on a 1.5 T clinical system, using a TLE protocol that included a whole-brain three-dimensional volumetric acquisition sequence, in addition to standard axial and sagittal sequences. The volumetric sequence entailed ~124 contiguous T_1-weighted images. All images were reviewed by a neuroradiologist with a specific expertise in epilepsy studies.

Post-acquisition MR image processing

All post-acquisition imaging processing and analysis were performed by a single operator blinded to the post-surgical outcome. The images were loaded into a UNIX workstation running Analyze™ 6.0 (Mayo Foundation, Rochester, MN), and the DICOM format files were converted into Analyze 7.5 format. Raw 16-bit data was re-scaled to 8 bits, and the image was made cubic, with voxel size identical in all three dimensions before image analysis.

The steps involved in the imaging processing are summarized in Fig. 1. Initially the pre- and postoperative MR images were segmented using an automated morphological segmentation technique (Object Extractor) to define the brain surface and exclude extra-cerebral structures (Fig. 1, Step 2). A binary image of the segmented brain MRI was then constructed and interior 'holes' were deleted, and Step Editing and Image Algebra tools were used to further refine the extraction, filling holes and separating all brain from non-brain structures, on a slice-by-slice basis.

Using a brain surface-matching technique with Analyze 6.0, as has been previously described, the postoperative binary MRI was matched and transformed into the same three-dimensional space as the preoperative binary MRI (Hogan *et al.*, 1996; O'Brien *et al.*, 1998*a*). In brief, this involves 1000 points being sampled on the surface of the postoperative binary MRI, which are then matched to the corresponding points on the preoperative binary MRI. From this a matrix is calculated that describes the transformation of the postoperative binary MRI into the same three-dimensional space as the preoperative binary MRI (Fig. 1, Step 2). This transformed postoperative image was saved and the matrix used in this transformation was also applied to the postoperative volumetric grey scale MR image. The transformed postoperative grey scale image was surface-matched with the preoperative grey scale image, and the matrix manually refined, using multiple anatomical markers throughout the brain, to ensure an optimal registration. Particular attention was paid to the alignment of the superior temporal gyrus on the side of the resection to assess for, and minimize, any potential effects of brain shift on the calculation of the resected brain volume (Fig. 2). The transformed postoperative binary and grey scale images, and the matrix used in these transformations, were saved for later use.

Using region of interest (ROI) tools, the volume of temporal lobe resected was then calculated, including amygdala, hippocampus and parahippocampal gyrus in addition to temporal neocortex. This was performed in the sagittal plane, on a slice-by-slice basis, by tracing in a semi-automated manner the resection margins from the co-registered postoperative MRI and the brain surface edge on the preoperative MRI (Fig. 3). This ROI, defining the resected structures, was saved for use in the analysis of the proportion of the SPM-defined FDG-PET hypometabolism that was included in the resection.

The total cerebral volume was calculated from the preoperative binary MRI image using a volume render tool, and thus the percentage 'normalized' temporal MRI volume resected was calculated by

$$\text{Normalized temporal MRI volume resected} = \frac{\text{Temporal MRI volume resected}}{\text{Total MRI cerebral volume}} \times 100$$

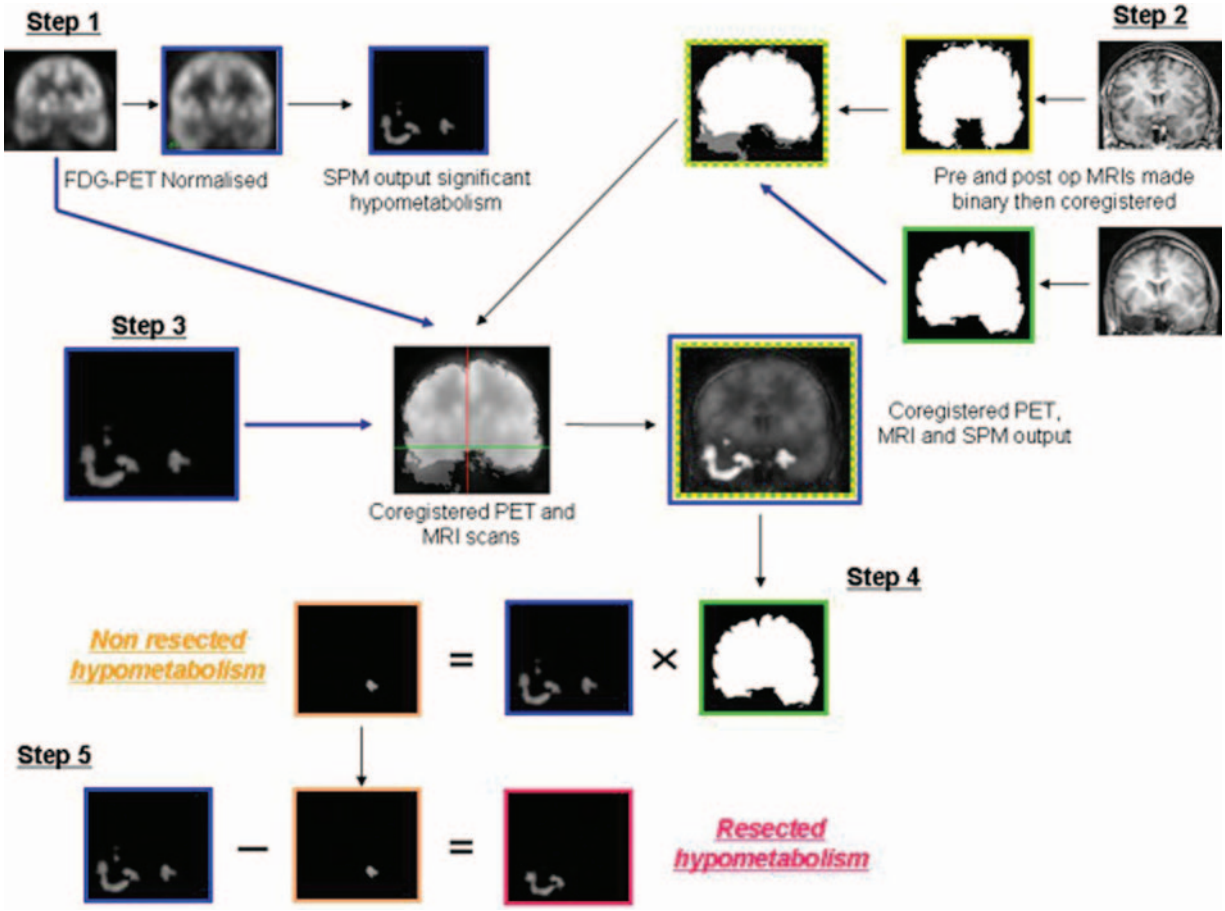

Fig. 1 Flow chart demonstrating the key steps in the post-acquisition image processing to calculate the resected and non-resected total brain hypometabolism. Step 1: FDG-PET scan normalized to the standard brain template and compared with 20 normal brains to identify the regions of significant hypometabolism. Step 2: The pre- and postoperative scans are made binary, and then the postoperative scan co-registered to the preoperative scan. Step 3: The SPM image and the FDG-PET scan are co-registered to the MRI scans. Step 4: Postoperative binary MRI scan multiplied by the SPM image to identify the non-resected SPM hypometabolism. Step 5: Non-resected SPM hypometabolism subtracted from the total SPM hypometabolism to calculate the resected SPM hypometabolism.

The region of the temporal lobe, including hippocampal and limbic structures as well as temporal neocortex was dissected from the extra-temporal brain structures, for later use in differentiating temporal from extra-temporal hypometabolism. Using Image Edit tools, the posterior margin of the temporal lobe on the preoperative volumetric MR image was defined in the sagittal plane. A straight line between the posterior margin of the sylvian fissure and the temporo-occipital incisure was used to define the posterior margin of the temporal lobe (Fig. 4A), and all cerebral structures posterior to this were deleted (Fig. 4B). The temporal lobe was then dissected from the brain in the coronal plane using a combination of manual and autotracing (Fig. 4C). All other cerebral structures were then deleted (Fig. 4D), and the volume of temporal lobe was calculated.

Post-acquisition FDG-PET image processing

Post-acquisition analysis was performed off-line with the aid of the software packages Analyze 6.0 (Mayo Foundation) and SPM99 (Wellcome Department of Cognitive Neurology, University College London, London, UK) implanted in MedX. FDG-PET images were converted from Interfile to Analyze 7.5 format, and then loaded into MedX. Images from patients and volunteers were then spatially normalized into standard PET templates provided in SPM99 using a 12-parameter affine transformation (Fig. 1, Step 1).

To remove the effect of global metabolism, the count of each voxel was normalized to the total count of the brain using proportional scaling. Threshold masking to remove signal from uptake in extra-cerebral structures was set at 40% for all patients. This level of thresholding was determined empirically as the optimal level for including hypometabolic zones but excluding non-brain structures before the performance of the analyses for this study.

This image was then compared with the 20 normalized volunteer FDG-PET scans, using an unpaired *t*-test, and significant regions of hypometabolism were identified (Fig. 5). Regions considered significant were cluster sizes larger than 200 contiguous voxels, with an uncorrected P-value < 0.0005. This SPM output image was then saved for future use (Fig. 1, Step 1).

The normalized FDG-PET was then transformed back into its original three-dimensional space in MedX using the original FDG-PET image as the template. The matrix generated was then applied to the SPM output image to transform it from the dimensions of the standard template into those of the patient's original FDG-PET image (Fig. 1, Step 1). This image was then co-registered and transformed to the preoperative binary MRI with surface-matching

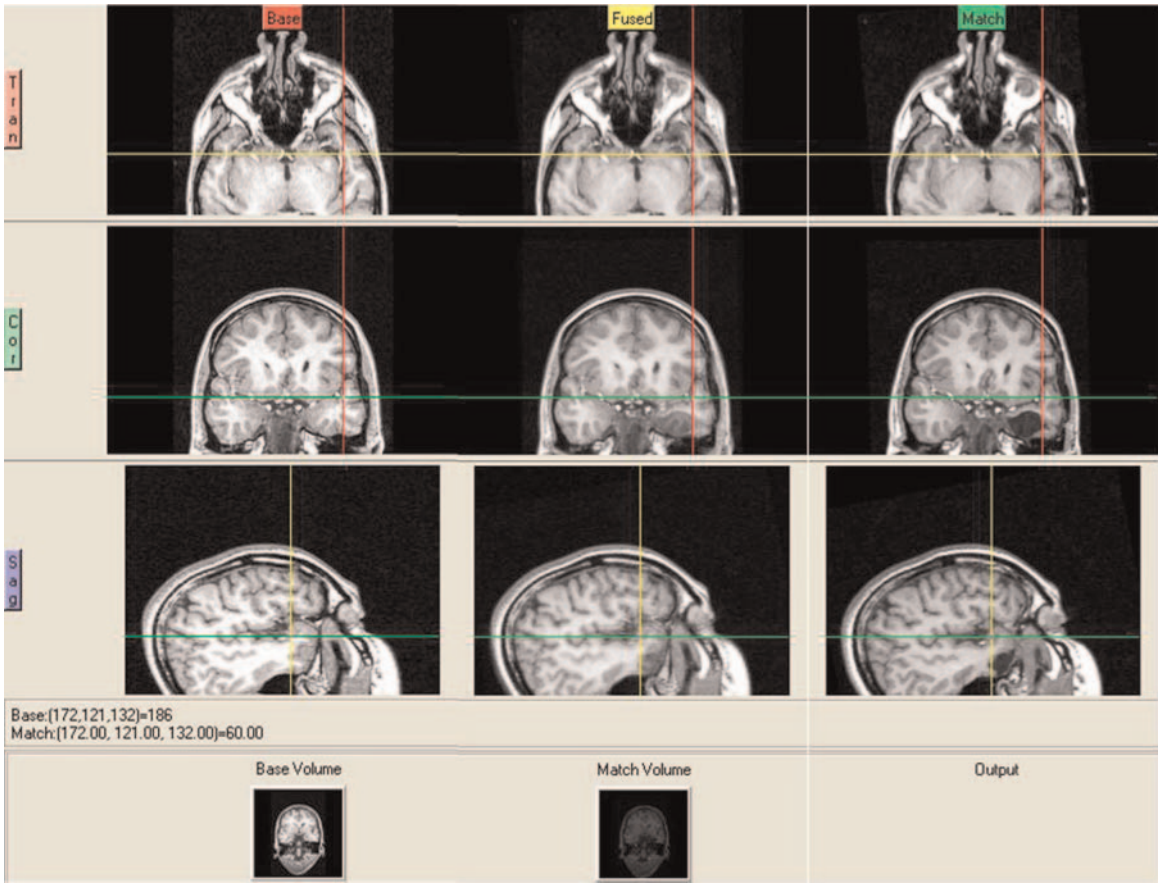

Fig. 2 Example of co-registration and rigid body 3D transformation of the postoperative MR (left) to the preoperative MR (right) image sets. Following the automated surface-matching registration, manual adjustment was performed using multiple anatomical markers throughout the brain to ensure an optimum alignment of the pre- and postoperative MR images. Particular attention was paid to the alignment of the superior temporal gyrus (location demonstrated by intersecting markers) to ensure that there was no significant postoperative brain shift that may affect the calculation of the resected temporal lobe volume.

utilizing the original FDG-PET image as the template to construct the matrix (Fig. 1, Step 3).

The binary image of the segmented transformed postoperative MRI scan was then multiplied by the transformed SPM hypometabolism image to produce an image containing only the voxels in which the hypometabolism was located within non-resected brain (Fig. 1, Step 4). Subtracting this 'non-resected SPM hypometabolism' image from the total transformed SPM output created an image of the hypometabolic voxels that lay within the region of temporal lobe that was resected ('resected SPM hypometabolism') (Fig. 1, Step 5). The volume of the resected SPM hypometabolism and the non-resected SPM hypometabolism was then calculated and expressed as a percentage of the total brain SPM hypometabolism volume. The percentage of the total volume of hypometabolism resected was then calculated by (Fig. 6):

$$\%\ \text{Volume SPM hypometabolism resected} = \frac{\text{Volume SPM hypometabolism resected}}{\text{Total volume of SPM hypometabolism}} \times 100$$

In addition to the volume of total hypometabolism resected, the volume of temporal and of extra-temporal hypometabolism present on the transformed SPM output image and the percentage of the temporal lobe hypometabolism resected were also calculated. The ROI defining the temporal lobe from the preoperative MRI was made binary (Fig. 7, Step1) and multiplied by the transformed SPM image to produce an image containing only the voxels in which the hypometabolism was located within the temporal lobe ('temporal SPM hypometabolism') (Fig. 7, Step 2). Subtracting this temporal SPM hypometabolism image from the total transformed SPM output created an image of the hypometabolic voxels that lay outside the regions of temporal lobe ('extra-temporal SPM hypometabolism') (Fig. 7, Step 3).

The 'temporal SPM hypometabolism' image was also multiplied by the binary MRI-derived 'temporal resection' image, to produce an image of the region of significant hypometabolism in the resected portion of the temporal lobe (Fig. 7, Step 4). This enabled calculation of the percentage of the temporal hypometabolism resected and its relationship to outcome.

The proportion of the resected hypometabolism that was in the medial temporal area was also calculated. For this the preoperative MRI scan was loaded into ROI tool in Analyze, with the co-registered SPM output of the 'resected SPM hypometabolism' loaded as a related volume. An ROI square was placed over the mesial temporal structures, including the hippocampus and amygdala on the preoperative MRI, and the volume of the cluster

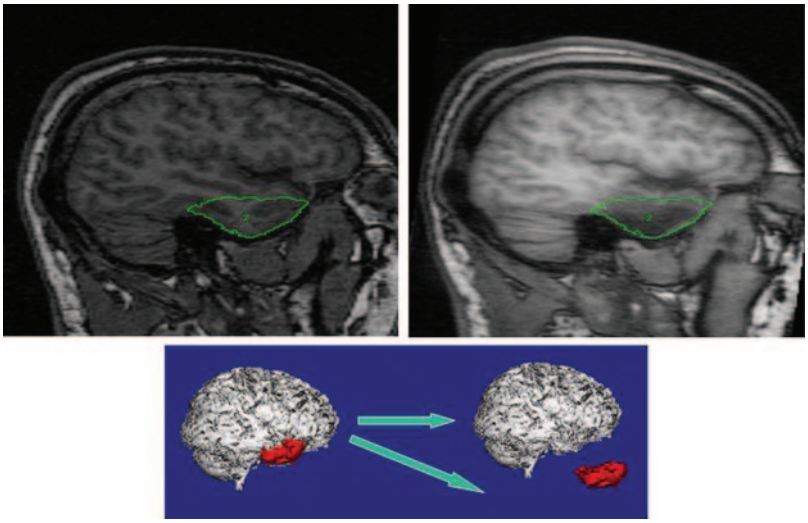

Fig. 3 Method for calculation of the volume of temporal lobe resected. The resected temporal lobe is traced on the preoperative MRI scan using the co-registered postoperative MRI as a template for the posterior resection margins.

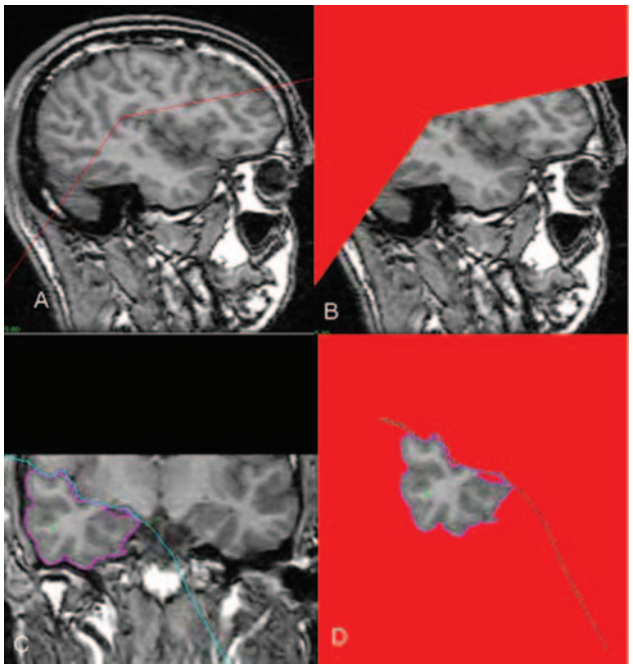

Fig. 4 Method used to determine the temporal lobe volume. (**A**) In the sagittal plane, a line is connected from the posterior margin of the sylvian fissure to the temporo-occipital incisure. (**B**) All cerebral and extra-cerebral structures posterior to this are deleted. (**C**) Image is then converted to the coronal plane, and using semi-automated tracing, the temporal lobe is identified. (**D**) All other structures are deleted.

of the SPM output in this region was measured. The proportion of the total volume of resected hypometabolism that this represented was then determined (i.e. % resected hypometabolism in the medial temporal area).

To determine whether the anatomical site of the unresected hypometabolism had an influence on outcome, the SPM output image was co-registered and fused with the patient's preoperative MRI scan. This image was then visually assessed, and the presence of hypometabolism in 12 defined regions of the brain was documented (Table 4).

Statistical analysis

Statistical analysis was performed with the aid of the software package Stata 8.0. Patients with a good versus poor post-surgical outcome were compared for the following variables initially with a univariate analysis using a two-tailed Student's *t*-test: (i) the percentage of the total brain SPM hypometabolism resected; (ii) the volume of the total brain SPM hypometabolism present; (iii) the percentage of temporal lobe SPM hypometabolism resected; (iv) the volume of temporal and extra-temporal lobe SPM hypometabolism present; (v) the percentage of the resected SPM hypometabolism that lay in the medial temporal area; (vi) the normalized volume of MRI-defined temporal lobe resected; and (vii) the percentage of total MRI-defined temporal lobe this volume represents. The variables that had a P-value < 0.1 on the univariate analysis were entered into a multivariate regression analysis to determine the independent contributions of each variable to post-surgical outcome. The proportion of patients in the good and poor surgical outcome groups who had unresected hypometabolism affecting each of the 12 brain regions was compared with a Fisher's exact test. For all tests $P < 0.05$ was considered a statistically significant difference between the groups.

Results

Clinical details and post-surgical outcome

The cohort consisted of 13 males and 13 females with a mean age of 42 (range: 22–69). HS was present on the preoperative MRI in 18 (69%) of the 26 patients. The remaining eight (31%) patients had normal preoperative MRIs, with no lesion present in either temporal lobe. Histopathology of the resected temporal lobes confirmed HS in all 18 MRI-defined HS patients. The remaining eight (31%) patients with normal MRIs had no specific abnormality identified on

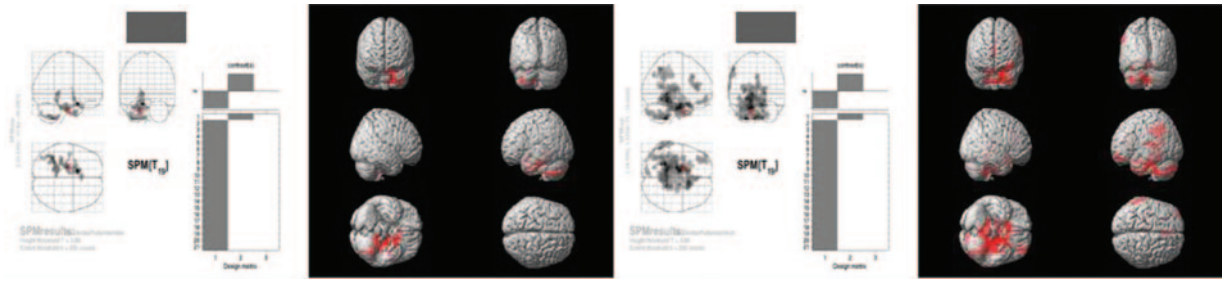

Fig. 5 SPM output images showing the regions of significant FDG-PET hypometabolism from two patients. The image on the left is from a patient in the good outcome group and displays hypometabolism that is restricted to the left temporal lobe. The image on the right is from a patient in the poor outcome group and displays more widespread hypometabolism involving extra-temporal and temporal regions.

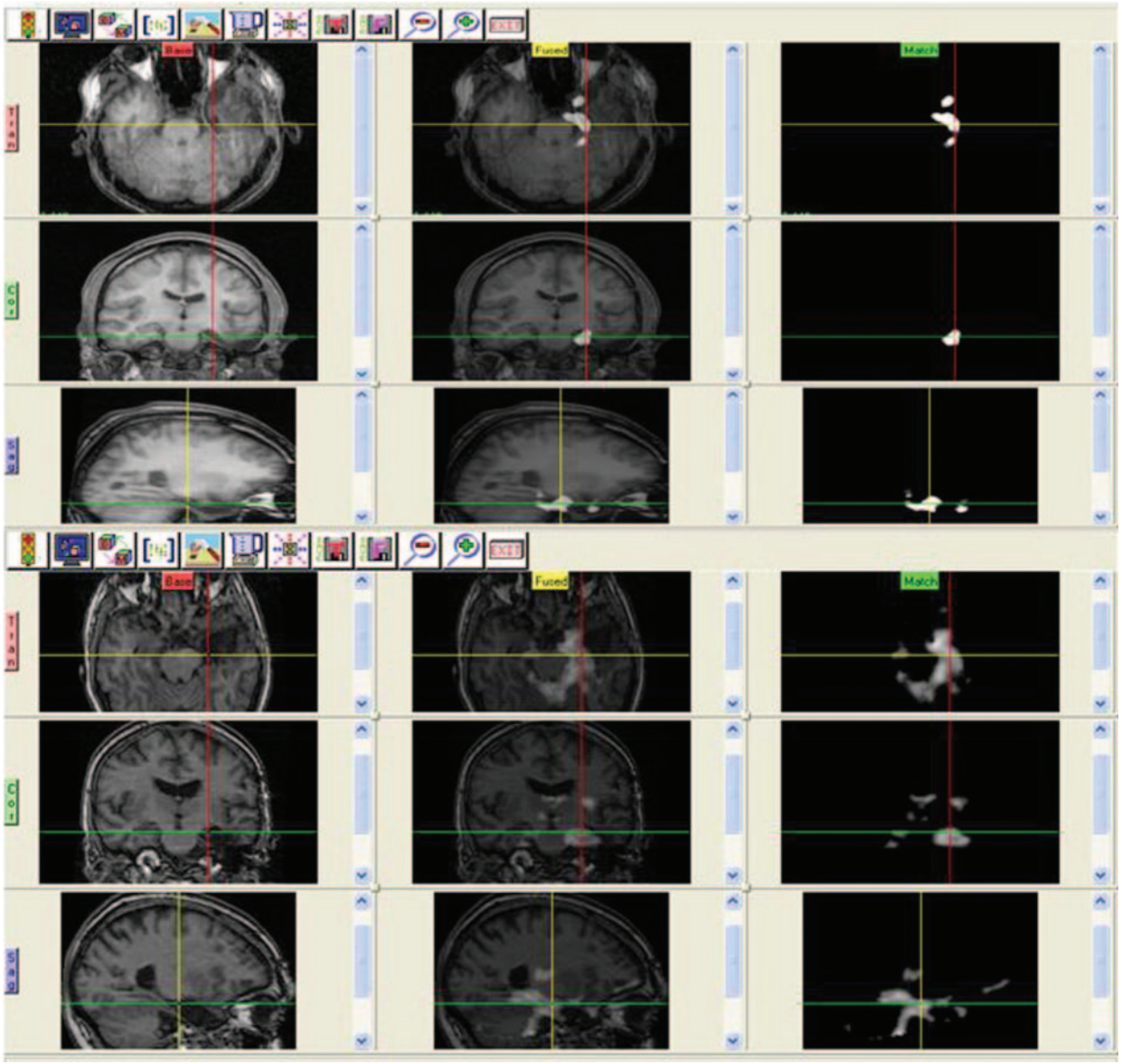

Fig. 6 Examples of method for calculating the percentage of hypometabolism resected: co-registering the postoperative MRI with the SPM output of significant areas of hypometabolism allowed a calculation of the proportion of the hypometabolism resected. The top image is from a patient in the good outcome group (same patient as for the left image in Fig. 5), with 30% of the hypometabolism resected. The bottom image is from a patient in the poor outcome group (right image in Fig. 5), with only 16% of the hypometabolism resected.

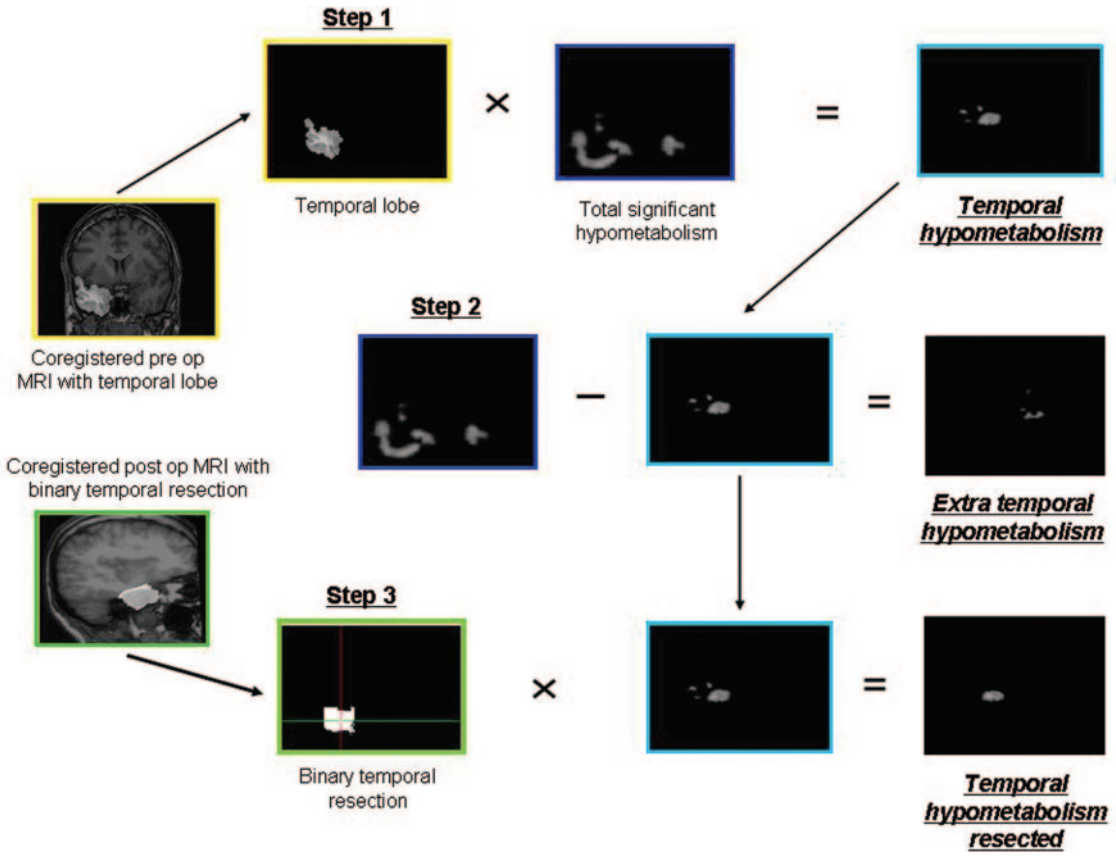

Fig. 7 Flow chart demonstrating the key steps in calculating the volume of temporal, extra-temporal and resected temporal SPM-defined hypometabolism. Step 1: Entire temporal lobe dissected from the preoperative MRI and a binary image of this then multiplied by total co-registered and transformed SPM-defined hypometabolism to determine the temporal SPM hypometabolism. Step 2: Temporal SPM hypometabolism subtracted from total brain SPM hypometabolism to reveal extra-temporal SPM hypometabolism. Step 3: Temporal SPM hypometabolism multiplied by binary temporal resection image to reveal the temporal SPM hypometabolism resected.

histopathological examination. Mean post-surgical follow-up was 4.5 years (range: 2.5–6.9 years). Median seizure frequency score preoperatively was 8 (range: 7–10). Median seizure frequency score at last postoperative follow-up was 4 (range: 2–8), and the median change in seizure score from pre- to post-surgery was 3 (range: 0–7). Of the 26 patients, 15 patients (58%) had a good outcome, and 11 (42%) had a poor outcome. The clinical details of the patients are summarized in Table 2. Of the four patients who had subdural grids implanted before surgery, one had a good outcome and three had a poor outcome. All these patients had hypometabolism on the FDG-PET scan extending beyond the ictal onset zone recorded on the subdural grids into extra-temporal regions. As the extent of coverage by the subdural grids was relatively restricted, it was not possible to make a useful assessment of the topographic relationship between the regions of hypometabolism and regions of seizure spread.

At last follow-up the median number of AEDs was 1 (range: 1–2) in the good outcome group and 2 (range: 1–4) in the poor outcome group.

Relationship of surgical outcome to extent of total FDG-PET resection and temporal lobe FDG-PET resection

The results of the univariate analysis comparing the SPM-defined FDG-PET hypometabolism resection and MRI volume of temporal lobe resection variables to the post-surgical outcome are summarized in Table 3. Patients with a good outcome had a greater proportion of the hypometabolism volume resected than those with a poor outcome (24.0% versus 11.7%, $P = 0.02$, Student's t-test). There was no significant difference between the groups in the total brain volume ($P = 0.84$) of hypometabolism present.

There was no significant difference between the outcome groups in the volume of the SPM-defined region of hypometabolism within the temporal lobe. The mean percentage of hypometabolism within the temporal lobe that was resected was also not significantly different in the good outcome group (41.8%, range: 0–60.5%) compared with the poor outcome group (33.7%, range: 0–63.8%,) ($P = 0.32$, Student's t-test). The volume of extra-temporal hypometabolism, whilst not statistically significant ($P = 0.07$),

showed a trend towards a larger volume of extra-temporal hypometabolism in the poor outcome group.

The percentage of the resected temporal hypometabolism that lay within the medial temporal areas was also analysed, and there was no significant difference between patients in the good outcome group (mean: 48.5% ± 9.2) and the poor outcome groups (mean: 38.5% ± 11.4) ($P = 0.5$, Student's *t*-test).

When the brain sites of the unresected hypometabolism were compared between the two outcome groups, there was no region in which the frequency of involvement significantly differed between them (Table 4).

Relationship of surgical outcome to volume of temporal lobe resected

The MRI-derived volume of temporal lobe resected was calculated to assess the effect of resection size on outcome. The mean temporal volume resected in the good outcome group was 27.6×10^3 mm^3 (range: 10.6×10^3 mm^3 to 40.4×10^3 mm^3), which did not differ from that in the poor outcome group of 27.7×10^3 mm^3 (range: 11.3×10^3 mm^3 to 41.9×10^3 mm^3) ($P = 0.97$). The volume of temporal lobe resected was normalized for the patient's total cerebral volume before comparison. In addition, the percentage of total temporal volume resected was calculated. In the good outcome group the mean percentage of temporal volume resected was 35.32% (range: 14.33–44.76%), which also did not differ significantly from that in the poor outcome group (31.5%, range: 13.6–45.83%, $P = 0.32$).

Nine of the 15 patients in the good outcome group and 5 of the 11 patients in the poor outcome had right-sided temporal lobectomies. When comparing side of resection and volume of resection, there was no significant difference in the volume resected between left- and right-sided procedures ($P = 0.69$, Student's *t*-test).

Table 2 Clinical features of patients in study

	Good outcome ($n = 15$)	Poor outcome ($n = 11$)
No of males, no of females	7, 8	6, 5
Mean age (years)	39	44
Number with MTS (%)	13 (87%)	5 (45%)
Side of surgery (R/L)	9R, 6L	5R, 6L
Time since surgery (years)	4.1	5.3

Multiple regression analysis

The results of the multiple regression analysis are summarized in Table 5. Variables with a *P*-value < 0.1 on the univariate analysis were included as independent variables (i.e. % total volume hypometabolism resected, extra-temporal volume hypometabolism and presence of HS on the preoperative MRI), with post-surgical outcome being the dependent variable. This analysis demonstrated that the extent of resection of the hypometabolism ($P = 0.049$) and the presence of HS ($P = 0.03$) were both independently predictive of outcome. Although the extra-temporal volume of hypometabolism showed a trend to significance on the univariate analysis, the multiple regression demonstrates that this was not independently associated with outcome.

Discussion

Temporal lobectomy has been established as a proven, effective treatment for medically refractory TLE, with most series reporting that ~70% of patients achieve an Engel Class I and II outcome, although reported rates vary from 33 to 93% (McIntosh *et al.*, 2001). Selection of patients for epilepsy surgery involves utilizing multiple diagnostic tests to adequately localize the epileptogenic zone preoperatively. However, even in carefully selected patients, a significant proportion of patients continue to have seizures. Preoperative prognostic indicators are therefore important in identifying suitable surgical candidates, and in providing pre-surgical outcomes and counselling.

Various studies have aimed to determine whether individual investigations, specifically FDG-PET, MRI, Wada's test, SPECT and electroencephalography, can accurately predict seizure freedom after surgery (Jeong *et al.*, 1999; Gilliam *et al.*, 2000; Clusmann *et al.*, 2002; Stavem *et al.*, 2004). The presence of HS or a structural lesion visible on MRI has been repeatedly shown to be associated with a better surgical outcome (Jack *et al.*, 1992, 1995; Berkovic *et al.*, 1995; Jeong *et al.*, 1999; Gilliam *et al.*, 2000; Clusmann *et al.*, 2002; Stavem *et al.*, 2004). Other clinical factors have also been investigated, such as duration

Table 3 Univariate analysis comparing the imaging variables with the outcomes from surgery

	Good outcome	Poor outcome	*P*-value
% Total volume hypometabolism resected (mean ± SEM)	24.1 ± 4.2%	11.8 ± 2.7%	$P = 0.02$
Total brain volume of hypometabolism (mm^3) (mean ± SEM)	$1.40 \times 10^5 \pm 0.4 \times 10^5$	$1.51 \times 10^5 \pm 0.4 \times 10^5$	$P = 0.84$
Temporal lobe volume of hypometabolism (mm^3) (mean ± SEM)	$0.23 \times 10^5 \pm 0.04 \times 10^5$	$0.24 \times 10^5 \pm 0.06 \times 10^5$	$P = 0.89$
Extra-temporal volume of hypometabolism (mm^3) (mean ± SEM)	$0.79 \times 10^5 \pm 0.12 \times 10^5$	$1.42 \times 10^5 \pm 0.45 \times 10^5$	$P = 0.07$
% Temporal hypometabolism resected (mean ± SEM)	41.8 ± 4.8%	33.7 ± 7.3%	$P = 0.32$
% Resected hypometabolism in the medial temporal area (mean ± SEM)	48.5 ± 9.15%	38.5 ± 11.40%	$P = 0.50$
Temporal MRI volume resected (mm^3)	$0.28 \times 10^5 \pm 0.02 \times 10^5$	$0.28 \times 10^5 \pm 0.04 \times 10^5$	$P = 0.99$
HS on MRI	13 (87%)	5 (45%)	$P = 0.03$
Right versus left temporal lobectomy	9R:6L	5R:6L	$P = 0.69$

Table 4 Location of unresected hypometabolism

Location of unresected hypometabolism	Good = 15	Poor = 11	*P*-value*
IPS posterior temporal lobe	9 (60%)	7 (64%)	0.59
IPS frontal lobe	9 (60%)	8 (73%)	0.40
IPS parietal lobe	4 (27%)	1 (9%)	0.27
IPS occipital lobe	1 (0.7%)	0 (0%)	0.58
IPS basal ganglia	6 (40%)	7 (64%)	0.21
IPS cerebellum	7 (47%)	8 (73%)	0.18
CL posterior temporal lobe	4 (27%)	5 (45%)	0.28
CL frontal lobe	4 (27%)	6 (55%)	0.15
CL parietal lobe	2 (13%)	1 (9%)	0.62
CL occipital lobe	1 (0.7%)	0 (0%)	0.58
CL basal ganglia	8 (53%)	5 (45%)	0.50
CL cerebellum	4 (27%)	7 (64%)	0.07

IPS = ipsilateral to side of resection; CL = contralateral to side of resection.
*Fisher's exact test.

Table 5 Multiple regression analysis model for post-surgical outcome

Independent variable	Postoperative outcome[a] (R^2 = 0.39, P = 0.011)		
	Beta	SE	*P*-value
MRI[b]	0.39	0.17	0.03
% Hypometabolism resected[c]	−0.37	0.18	0.049
Vol extra-temporal hypometabolism[d]	0.15	0.18	0.41

R^2 = *R*-square (the coefficient of multiple determination) of the model; Beta = standardized regression coefficients for each independent variable; SE = standard error for each independent variable.
[a]Postoperative outcome: (i) good (i.e. seizure frequency score ⩽ 5); (ii) localization non-concordant or non-localizing. [b]MRI groups: (i) mesial temporal sclerosis; (ii) normal MRI. [c]% SPM resected: percentage of the total volume of hypometabolism resected. [d]Vol SPM extra-temporal: volume of extra-temporal hypometabolism (mm^3).

of seizures before surgery, IQ, presence of only partial seizures and a history of febrile convulsions, with no consistent relationship to surgical outcome being demonstrated (Chelune *et al.*, 1998; Clusmann *et al.*, 2002; Stavem *et al.*, 2004). One study demonstrated that in addition to the presence of HS, age at surgery was also a prognostic factor, suggesting that mesial TLE may be a progressive disorder, and early surgical intervention should be considered (Jeong *et al.*, 1999).

FDG-PET is accepted as a sensitive and specific tool for the localization of epileptogenic zones in TLE, with rare false lateralization (Sperling *et al.*, 1995). Cerebral glucose uptake is believed to reflect the overall strength of synaptic activity (Knowlton *et al.*, 2001). The interictal hypometabolism evident on FDG-PET scanning in epileptogenic temporal lobes is a common finding in TLE, and present in >80% of patients (Lee *et al.*, 2002). The reasons for the decreased glucose metabolism are unknown. It is unclear whether this loss of synaptic activity is a result of neuronal cell death, or metabolic dysfunction of the underlying neurons.

HS is characterized pathologically by loss of neurons in the hilus and CA1 subfield of the hippocampus. The cell loss results in hippocampal atrophy, which can be reliably assessed with quantitative MRI, and the degree of atrophy has been shown to correlate well with the degree of neuronal cell loss (Cascino *et al.*, 1991; Lee *et al.*, 1995). It has been proposed that the hypometabolism seen on FDG-PET is a reflection of the underlying neuronal cell loss seen in HS. A recent study found that hippocampal atrophy and presumed degree of cell loss appears to be a factor involved in the aetiology of the hypometabolism in epileptogenic hippocampi (Knowlton *et al.*, 2001). However, this finding is not consistent with other studies demonstrating temporal hypometabolism occurring in the absence of hippocampal atrophy (Lamusuo *et al.*, 2001; O'Brien *et al.*, 2001; Carne *et al.*, 2004). Many other studies have found that the degree of hypometabolism does not correlate well with the severity of neuronal cell loss (Radtke *et al.*, 1993; O'Brien *et al.*, 1997; Lamusuo *et al.*, 2001; Theodore *et al.*, 2001), and that the severity of hypometabolism may not relate to post-surgical outcome (Lee *et al.*, 2002). Hypometabolism in TLE is also frequently seen to extend outside the hippocampal structures, where atrophy is not present (Koutroumanidis *et al.*, 2000; Newberg *et al.*, 2000; Choi *et al.*, 2003), and the extent of the hypometabolism is also typically much larger than the histopathological or MRI abnormality (Semah *et al.*, 1995). There is now evidence that hypometabolism may reflect physiological dysfunction of the underlying temporal lobe and functionally associated regions, rather than just neuronal cell loss (Hong *et al.*, 2002; Lamusuo *et al.*, 2001; Lee *et al.*, 2002; Vielhaber *et al.*, 2003). Repeated seizures can result in synaptic reorganization, with neuronal sprouting and proliferation in glial cells, and this may underlie the metabolic changes seen on FDG-PET. Furthermore, one study has demonstrated improvement in both the ipsilateral and contralateral glucose metabolism in the temporal neocortex after epilepsy surgery (Hajek *et al.*, 1994), which would be consistent with a physiological dysfunction as the cause for the hypometabolism, rather than just cell loss.

The pattern of hypometabolism seen on the preoperative FDG-PET scan has also been examined as a prognostic indicator. The presence of ipsilateral temporal hypometabolism has been found to correlate with higher rates of seizure freedom postoperatively (Radtke *et al.*, 1993; Manno *et al.*, 1994; O'Brien *et al.*, 2001). However, it has been observed that the presence of extra-temporal cortical hypometabolism, as well as contralateral, bitemporal or thalamic hypometabolism, all have poorer seizure freedom rates post-temporal lobectomy (Koutroumanidis *et al.*, 2000; Newberg *et al.*, 2000; Choi *et al.*, 2003).

This current study is the first to examine whether the extent of resection of the region of FDG-PET hypometabolism is correlated with post-surgical outcome. The results show that a greater extent of surgical excision of the total region of cerebral hypometabolism, as defined by SPM analysis, is associated with a better postoperative outcome. Furthermore,

this was demonstrated to be independent of the total amount of hypometabolism present. We also compared the total volume of temporal hypometabolism, and the percentage of this that was resected, between the outcome groups but found no significant differences. In light of previous findings regarding the presence of extra-temporal hypometabolism being associated with a poorer outcome (Koutroumanidis *et al.*, 2000; Newberg *et al.*, 2000; Choi *et al.*, 2003), we compared the volume of extra-temporal hypometabolism between the outcome groups. While there was a trend ($P = 0.07$) on the univariate analysis for the volume of extra-temporal hypometabolism to be greater in the poor outcome group (Table 3), on the multivariate regression analysis this was not independently associated with outcome (Table 5). This would suggest that the presence of extra-temporal or contralateral hypometabolism *per se* is not the poor prognostic factor, but rather it is the percentage of the total amount of hypometabolism available for resection that is associated with outcome. Patients with more extensive extra-temporal hypometabolism are more likely to have a smaller proportion of the total volume of hypometabolism in the brain resected, which may explain the previously reported association of outcome with this variable. Our results would suggest that the presence of small areas of hypometabolism in extra-temporal regions, regardless of where they are, may not preclude a good outcome, provided that a significant proportion of the total hypometabolism was in the ipsilateral temporal lobe, and accessible for surgical resection. These findings are consistent with the hypothesis that the hypometabolism is a result of underlying epileptogenically induced metabolic dysfunction, and that resecting a greater portion results in improved rates of seizure freedom, irrespective of its total volume. Further support for this view is provided in the analysis demonstrating no significant differences between the outcome groups in the proportion of patients in whom the unresected hypometabolism involved any of the 12 brain regions examined (Table 4).

It is clear from the findings of our study that complete removal of the hypometabolic area is not a prerequisite for a good postoperative outcome. The patients in the good outcome group had an average of only 24% of the total region of brain hypometabolism resected. Further studies with a larger patient cohort would be interesting for subgroup analysis to assess if the relationship between percentage hypometabolism resected and postoperative seizure frequency score are linearly related. From our results to date we postulate that resection of a critical volume of hypometabolism is associated with seizure freedom; however, the exact proportion required in each patient remains to be determined. Whilst our findings support the concept of the hypometabolism representing neuronal dysfunction, it is unclear why resection of only a portion can result in seizure freedom. It is possible that the hypometabolism is of varying severity in different regions of the brain and that this may represent differing degrees of underlying neuronal dysfunction. The hypometabolism in the temporal lobe may be different in severity from extra-temporal regions, which would be consistent with the concept of more severe neuronal dysfunction in the epileptogenic zone, than in extra-temporal and functionally associated regions. Tailoring resection margins based on the extent and severity of temporal hypometabolism (a 'PETectomy') would be an attractive option if it could be demonstrated that this yields improved seizure control rates (through resecting a greater percentage of dysfunctional neuronal tissue) and reduced neurophysiological deficit (through not resecting functional neuronal tissue).

The use of SPM and co-registration techniques in this study enabled the extent of resection of the region of significant hypometabolism to be quantified in a way that removed the inter-observer variability inherent in the visual interpretation of FDG-PET scans. To our knowledge such techniques have not been previously applied to address this research question. The findings of this study may have implications in patient selection, preoperative assessment and patient counselling regarding the likelihood of achieving seizure freedom after temporal lobectomy.

The relationship between the extent of surgical resection of the temporal lobe and postoperative outcome was also examined in this study using quantitative, MRI-based, methods. With the advances in neuroimaging and surgical techniques over time, differing surgical procedures have evolved, with considerable variation between epilepsy centres. A standard ATL remains the most widely performed operative procedure for TLE, and includes removal of the neocortical structures plus amygdalohippocampectomy (AH). However, there is no consensus on the amount of neocortical resection that is required to achieve the optimal outcome. It has been believed that a common cause of failed temporal lobectomy is inadequate hippocampal resection, and thus many surgeons endeavour to maximize the extent of hippocampal resection in an effort to improve post-operative seizure freedom. Hippocampal resection length has been examined as a prognostic indicator, and a more extensive hippocampal resection has been shown to produce higher rates of seizure freedom (Wyler *et al.*, 1995; Bonilha *et al.*, 2004; Stavem *et al.*, 2004). However, this finding is in contrast with other studies that have not demonstrated any relationship between outcome and the size of hippocampal resection (McKhann *et al.*, 2000).

Selective AH has become a popular surgical treatment option for mesial TLE in some centres. This procedure spares the lateral neocortical structures and has been used in an effort to reduce side-effects and post-surgical memory decline. Postoperative seizure freedom rates of selective AH have been shown to be comparable with more extensive temporal resections (Arruda *et al.*, 1996; Clusmann *et al.*, 2002). Previous studies have not demonstrated any clear relationship between the posterior extent of the neocortical resection and outcome following an ATL (Cascino *et al.*, 1995; Tran *et al.*, 1995; Malla *et al.*, 1998). However, many centres still use intra-operative electrocorticography to guide

the extent of the neocortical resection, potentially confounding this analysis. Furthermore, most seizure recurrences following temporal lobectomy have been shown to arise in the residual temporal neocortex (Hennessy *et al.*, 2000). To our knowledge, the volume of temporal lobe resected has not been quantified and analysed with respect to post-operative seizure freedom after surgery for TLE. In this study, all patients underwent standard ATL, performed by two different neurosurgeons. Electrocorticography was not used to guide the extent of the resection. The calculations of the volume of resection in our study were made after co-registering pre- and postoperative MRI scans, which enabled accurate assessment not only of the exact resection margins but also the volume of temporal lobe within those margins in each patient. The temporal lobe volume was also normalized for each patient's total cerebral volume before analysis, allowing for individual differences in brain volume. There was marked variability in the volume of tissue resected (1096–4193.78 mm^3). Despite this, no relationship between the volume of temporal lobe resected and outcome was found.

It is interesting to note that we did not find a significant difference between the good and bad outcome groups in the proportion of the resected hypometabolism that was in the medial temporal lobe (Table 3). It might be expected that if selective AH truly yields the same outcome results as standard ATL, most of the resected hypometabolism would reside within the medial temporal region. This result may therefore suggest that, in certain patients, resection of the anterior temporal structures—if affected by hypometabolism—may be required to optimize the chances of postoperative seizure control.

Conclusions

This study has demonstrated that the percentage of total volume of the region of cerebral hypometabolism on a preoperative FDG-PET image, as defined using SPM, that is included within the surgical resection is associated with post-surgical outcome. This was independent of the total volume of cerebral hypometabolism that is present, the presence of HS on histopathological examination and the volume of the temporal lobe resected. These approaches warrant further evaluation towards individualized surgical planning based on a combination of anatomical and functional imaging data.

References

Arruda F, Cendes F, Andermann F, Dubeau F, Villemure JG, Jones-Gotman M, et al. Mesial atrophy and outcome after amygdalohippocampectomy or temporal lobe removal. Ann Neurol 1996; 40: 446–50.

Berkovic SF, McIntosh AM, Kalnins RM, Jackson GD, Fabinyi GC, Brazenor GA, et al. Preoperative MRI predicts outcome of temporal lobectomy: an actuarial analysis. Neurology 1995; 45: 1358–63.

Bonilha L, Kobayashi E, Mattos JP, Honorato DC, Li LM, Cendes F. Value of extent of hippocampal resection in the surgical treatment of temporal lobe epilepsy. Arq Neuropsiquiatr 2004; 62: 15–20.

Carne RP, O'Brien TJ, Kilpatrick CJ, MacGregor LR, Hicks RJ, Murphy MA, et al. MRI-negative PET-positive temporal lobe epilepsy: a distinct surgically remediable syndrome. Brain 2004; 127: 2276–85.

Cascino GD, Jack CR Jr, Parisi JE, Sharbrough FW, Hirschorn KA, Meyer FB, et al. Magnetic resonance imaging-based volume studies in temporal lobe epilepsy: pathological correlations. Ann Neurol 1991; 30: 31–6.

Cascino GD, Trenerry MR, Jack CR Jr, Dodick D, Sharbrough FW, So EL, et al. Electrocorticography and temporal lobe epilepsy: relationship to quantitative MRI and operative outcome. Epilepsia 1995; 36: 692–6.

Chelune GJ, Naugle RI, Hermann BP, Barr WB, Trenerry MR, Loring DW, et al. Does presurgical IQ predict seizure outcome after temporal lobectomy? Evidence from the Bozeman Epilepsy Consortium. Epilepsia 1998; 39: 314–8.

Choi JY, Kim SJ, Hong SB, Seo DW, Hong SC, Kim BT, et al. Extratemporal hypometabolism on FDG PET in temporal lobe epilepsy as a predictor of seizure outcome after temporal lobectomy. Eur J Nucl Med Mol Imaging 2003; 30: 581–7.

Clusmann H, Schramm J, Kral T, Helmstaedter C, Ostertun B, Fimmers R, et al. Prognostic factors and outcome after different types of resection for temporal lobe epilepsy. J Neurosurg 2002; 97: 1131–41.

Engel J Jr, Van Ness PC, Rasmussen TB, Ojemann LM. Outcome with respect to epileptic seizures. In: Engel J Jr, editor. Surgical treatment of the epilepsies. New York: Raven Press; 1993. p. 609–21.

Gilliam F, Faught E, Martin R, Bowling S, Bilir E, Thomas J, et al. Predictive value of MRI-identified mesial temporal sclerosis for surgical outcome in temporal lobe epilepsy: an intent-to-treat analysis. Epilepsia 2000; 41: 963–6.

Griffith HR, Perlman SB, Woodard AR, Rutecki PA, Jones JC, Ramirez LF, et al. Preoperative FDG-PET temporal lobe hypometabolism and verbal memory after temporal lobectomy. Neurology 2000; 54: 1161–5.

Hajek M, Wieser HG, Khan N, Antonini A, Schrott PR, Maguire P, et al. Preoperative and postoperative glucose consumption in mesiobasal and lateral temporal lobe epilepsy. Neurology 1994; 44: 2125–32.

Hennessy MJ, Elwes RD, Binnie CD, Polkey CE. Failed surgery for epilepsy. A study of persistence and recurrence of seizures following temporal resection. Brain 2000; 123: 2445–66.

Henry TR, Babb TL, Engel J Jr, Mazziotta JC, Phelps ME, Crandall PH. Hippocampal neuronal loss and regional hypometabolism in temporal lobe epilepsy. Ann Neurol 1994; 36: 925–7.

Hogan RE, Cook MJ, Kilpatrick CJ, Binns DW, Desmond PM, Morris K. Accuracy of coregistration of single-photon emission CT with MR via a brain surface matching technique. AJNR Am J Neuroradiol 1996; 17: 793–7.

Hong SB, Han HJ, Roh SY, Seo DW, Kim SE, Kim MH. Hypometabolism and interictal spikes during positron emission tomography scanning in temporal lobe epilepsy. Eur J Neurol 2002; 48: 65–70.

Jack CR Jr, Sharbrough FW, Cascino GD, Hirschorn KA, O'Brien PC, Marsh WR. Magnetic resonance image-based hippocampal volumetry: correlation with outcome after temporal lobectomy. Ann Neurol 1992; 31: 138–46.

Jack CR Jr, Trenerry MR, Cascino GD, Sharbrough FW, So EL, O'Brien PC. Bilaterally symmetric hippocampi and surgical outcome. Neurology 1995; 45: 1353–8.

Jeong SW, Lee SK, Kim KK, Kim H, Kim JY, Chung CK. Prognostic factors in anterior temporal lobe resections for mesial temporal lobe epilepsy: multivariate analysis. Epilepsia 1999; 40: 1735–9.

Knowlton RC, Laxer KD, Klein G, Sawrie S, Ende G, Hawkins RA, et al. In vivo hippocampal glucose metabolism in mesial temporal lobe epilepsy. Neurology 2001; 57: 1184–90.

Koutroumanidis M, Hennessy MJ, Seed PT, Elwes RD, Jarosz J, Morris RG, et al. Significance of interictal bilateral temporal hypometabolism in temporal lobe epilepsy. Neurology 2000; 54: 1811–21.

Lamusuo S, Jutila L, Ylinen A, Kalviainen R, Mervaala E, Haaparanta M, et al. [^{18}F]FDG-PET reveals temporal hypometabolism in patients with temporal lobe epilepsy even when quantitative MRI and histopathological

analysis show only mild hippocampal damage. Arch Neurol 2001; 58: 933–9.

Lee N, Tien RD, Lewis DV, Friedman AH, Felsberg GJ, Crain B, et al. Fast spin-echo, magnetic resonance imaging-measured hippocampal volume: correlation with neuronal density in anterior temporal lobectomy patients. Epilepsia 1995; 36: 899–904.

Lee SK, Lee DS, Yeo JS, Lee JS, Kim YK, Jang MJ, et al. FDG-PET images quantified by probabilistic atlas of brain and surgical prognosis of temporal lobe epilepsy. Epilepsia 2002; 43: 1032–8.

Malla BR, O'Brien TJ, Cascino GD, So EL, Radhakrishnan K, Silbert P, et al. Acute postoperative seizures following anterior temporal lobectomy for intractable partial epilepsy. J Neurosurg 1998; 89: 177–82.

Manno EM, Sperling MR, Ding X, Jaggi J, Alavi A, O'Connor MJ, et al. Predictors of outcome after anterior temporal lobectomy: positron emission tomography. Neurology 1994; 44: 2331–6.

McIntosh AM, Wilson SJ, Berkovic SF. Seizure outcome after temporal lobectomy: current research practice and findings. Epilepsia 2001; 42: 1288–307.

McKhann GM II, Schoenfeld-McNeill J, Born DE, Haglund MM, Ojemann GA. Intraoperative hippocampal electrocorticography to predict the extent of hippocampal resection in temporal lobe epilepsy surgery. J Neurosurg 2000; 93: 44–52.

Newberg AB, Alavi A, Berlin J, Mozley PD, O'Connor M, Sperling M. Ipsilateral and contralateral thalamic hypometabolism as a predictor of outcome after temporal lobectomy for seizures. J Nucl Med 2000; 41: 1964–8.

O'Brien TJ, Newton MR, Cook MJ, Berlangieri SU, Kilpatrick C, Morris K, et al. Hippocampal atrophy is not a major determinant of regional hypometabolism in temporal lobe epilepsy. Epilepsia 1997; 38: 74–80.

O'Brien TJ, O'Connor MK, Mullan BP, Brinkmann BH, Hanson D, Jack CR, et al. Subtraction ictal SPET co-registered to MRI in partial epilepsy: description and technical validation of the method with phantom and patient studies. Nucl Med Commun 1998a; 19: 31–45.

O'Brien TJ, So EL, Mullan BP, Hauser MF, Brinkmann BH, Bohnen NI, et al. Subtraction ictal SPECT co-registered to MRI improves clinical usefulness of SPECT in localizing the surgical seizure focus. Neurology 1998b; 50: 445–54.

O'Brien TJ, So EL, Mullan BP, Cascino GD, Hauser MF, Brinkmann BH, et al. Subtraction peri-ictal SPECT is predictive of extratemporal epilepsy surgery outcome. Neurology 2000; 55: 1668–77.

O'Brien TJ, Hicks RJ, Ware R, Binns DS, Murphy M, Cook MJ. The utility of a 3-dimensional, large-field-of-view, sodium iodide crystal-based PET scanner in the presurgical evaluation of partial epilepsy. J Nucl Med 2001; 42: 1158–65.

Radtke RA, Hanson MW, Hoffman JM, Crain BJ, Walczak TS, Lewis DV, et al. Temporal lobe hypometabolism on PET: predictor of seizure control after temporal lobectomy. Neurology 1993; 43: 1088–92.

Semah F, Baulac M, Hasboun D, Frouin V, Mangin JF, Papageorgiou S, et al. Is interictal temporal hypometabolism related to mesial temporal sclerosis? A positron emission tomography/magnetic resonance imaging confrontation. Epilepsia 1995; 36: 447–56.

Sperling MR, Alavi A, Reivich M, French JA, O'Connor MJ. False lateralization of temporal lobe epilepsy with FDG positron emission tomography. Epilepsia 1995; 36: 722–7.

Stavem K, Bjornaes H, Langmoen IA. Predictors of seizure outcome after temporal lobectomy for intractable epilepsy. Acta Neurol Scand 2004; 109: 244–9.

Theodore WH, Newmark ME, Sato S, Brooks R, Patronas N, De La Paz R, et al. [^{18}F]Fluorodeoxyglucose positron emission tomography in refractory complex partial seizures. Ann Neurol 1983; 14: 429–37.

Theodore WH, Gaillard WD, De Carli C, Bhatia S, Hatta J. Hippocampal volume and glucose metabolism in temporal lobe epileptic foci. Epilepsia 2001; 42: 130–2.

Tran TA, Spencer SS, Marks D, Javidan M, Pacia S, Spencer DD. Significance of spikes recorded on electrocorticography in nonlesional medial temporal lobe epilepsy. Ann Neurol 1995; 38: 763–70.

Vielhaber S, Oertzen JH, Kudin AF, Schoenfeld A, Menzel C, Biersack H-J, et al. Correlation of hippocampal glucose oxidation capacity and interictal FDG-PET in temporal lobe epilepsy. Epilepsia 2003; 44: 193–9.

Wiebe S, Blume WT, Girvin JP, Eliasziw M. Effectiveness and Efficiency of Surgery for Temporal Lobe Epilepsy Study Group. A randomized, controlled trial of surgery for temporal-lobe epilepsy. N Engl J Med 2001; 345: 311–8.

Wyler AR, Hermann BP, Somes G. Extent of medial temporal resection on outcome from anterior temporal lobectomy: a randomized prospective study. Neurosurgery 1995; 37: 982–90; discussion 990–1.